Inst. Phys. Conf. Ser. No 141: Chapter 6
Paper presented at Int. Symp. Compound Semicond., San Diego, 18–22 September 1994

Strain-symmetrized $In_xGa_{1-x}As/In_yAl_{1-y}As$ HEMTs with extremely high 2DEG densities and mobilities

W. Klein, G. Böhm, H. Heiß, S. Kraus, D. Xu, R. Semerad, G. Tränkle, and G. Weimann

Walter-Schottky-Institut, Technische Universität München, D-85748 Garching, Germany

ABSTRACT: Strain-symmetrized $In_xGa_{1-x}As/In_yAl_{1-y}As$ heterostructures with $0.53 \leq x \leq 0.74$ and $0.52 \geq y \geq 0.415$ and enhanced 2DEG densities and mobilities were grown by molecular beam epitaxy on InP substrates. The increased conduction band offset resulted in extremely high electron densities of $3.81 \times 10^{12}\ cm^{-2}$, with a 4.2 K mobility of 51100 cm^2/Vs for single-sided doping and highest ever densities of $6.70 \times 10^{12}\ cm^{-2}$ for double-sided doping. The strain-symmetrization with stress compensating $In_yAl_{1-y}As$ barriers did not, however, allow an increase in the critical In content of the $In_xGa_{1-x}As$ QW.

1. Introduction

InGaAs/InAlAs high electron mobility transistors (HEMTs) on InP substrates are currently the most promising devices for high frequency amplification [1-5]. Device performance can be improved either by reducing the gate length [1,3] or by increasing the channel conductance [3,6-9]. The enhanced conduction band offset due to the increasing In content in the active channel leads to higher electron mobilities and saturation velocities. Numerous investigations have been made to maximize the In content in the channel [2,7,8], including stress compensated structures with opposite strain in quantum wells and barriers.

We investigated strain-symmetrized SQW structures with a homogeneously and compressively strained well and $In_yAl_{1-y}As$ under tensile strain for stress compensation. The essential advantages of these structures are a larger conduction band discontinuity due to the increased band gap in the $In_yAl_{1-y}As$ barrier, and a better pinch-off of the HEMTs due to improved electron confinement in the 12 nm wide QW. We demonstrate the optimization of 2DEG mobility and density in these structures with modified In contents in the barriers and the wells and, secondly, differing doping profiles. Optimized HEMT structures with single-sided and double-sided doping yielding 2DEG densities, measured at 4.2 K, as high as $3.81 \times 10^{12}\ cm^{-2}$ and $6.70 \times 10^{12}\ cm^{-2}$, respectively.

2. MBE growth

All structures used here were grown by solid source MBE on (100) oriented InP:Fe substrates with growth rates around 1 µm/h, a substrate temperature of 530 °C and a V/III ratio (beam equivalent pressure) of 27 . The different compositions of the ternary layers were obtained by controlling the group III flux ratio.

Figure 1 schematically shows the epitaxial layer sequence of the investigated HEMT structure. The buffer consists of two 100 nm thick $In_{0.52}Al_{0.48}As$ layers and two $In_{0.53}Ga_{0.47}As/In_{0.52}Al_{0.48}As$ superlattices. The temperatures of the Ga effusion cell was decreased while growing the second $In_{0.52}Al_{0.48}As$ layer from the value necessary for lattice matched growth to the value appropriate for the strained QW. The In flux was kept constant, except for the growth of the lattice matched cap layer. As our MBE machine is equipped with two Al cells (and a single Ga and In cell each), we were able to grow the layer sequence shown in Fig. 1 without any growth interruption at the QW interfaces, having different Al fluxes at our disposal.

The investigated range in the In contents of the QWs and the barriers are given in Table I. The Si doping level in the $In_yAl_{1-y}As$ supply layer was 1.5×10^{19} cm^{-3} for sample M5409, M5424 and M5425 and 1.0×10^{19} cm^{-3} for all others. The measured transport properties reflect the influence of the parallel conduction in the cap layers: Samples M5406 - M5410 have doped caps of only 7 nm thickness, whereas the other samples have thicker caps (5 nm undoped InGaAs topped by 10 nm doped InGaAs). The doping in the cap layers is 3.0×10^{18} cm^{-3} in all samples.

The characterization of our HEMT structures was made by Hall measurements at 300, 77 and 4.2 K and Shubnikov-de Haas (SdH) measurements at 4.2 K to separate the 2DEG conductance from the parallel conductance in the cap layers. The thicknesses of the surface

InGaAs $3\cdot10^{18}$ cm^{-3}	y=0.53	10 nm
InGaAs -	y=0.53	5 nm
InAlAs -	y=0.52	7 nm
InAlAs -	y=0.52 - 0.415	3 nm
InAlAs I-$1.5\cdot10^{19}$ cm^{-3}	y=0.52 - 0.415	12.5 nm
InAlAs -	y=0.52 - 0.415	2 nm
InGaAs -	y=0.53 - 0.74	12 nm
InAlAs -	y=0.52 - 0.415	6 nm
InAlAs 0-$1.5\cdot10^{19}$ cm^{-3}	y=0.52 - 0.415	2 nm
InAlAs -	y=0.52 - 0.415	16 nm
InAlAs -	y=0.52	100 nm
SL		
InAlAs -	y=0.52	100 nm
SL		
InP (:Fe) Substrat		

Figure 1: Schematic layer structure of a strain-symmetrized HEMT.

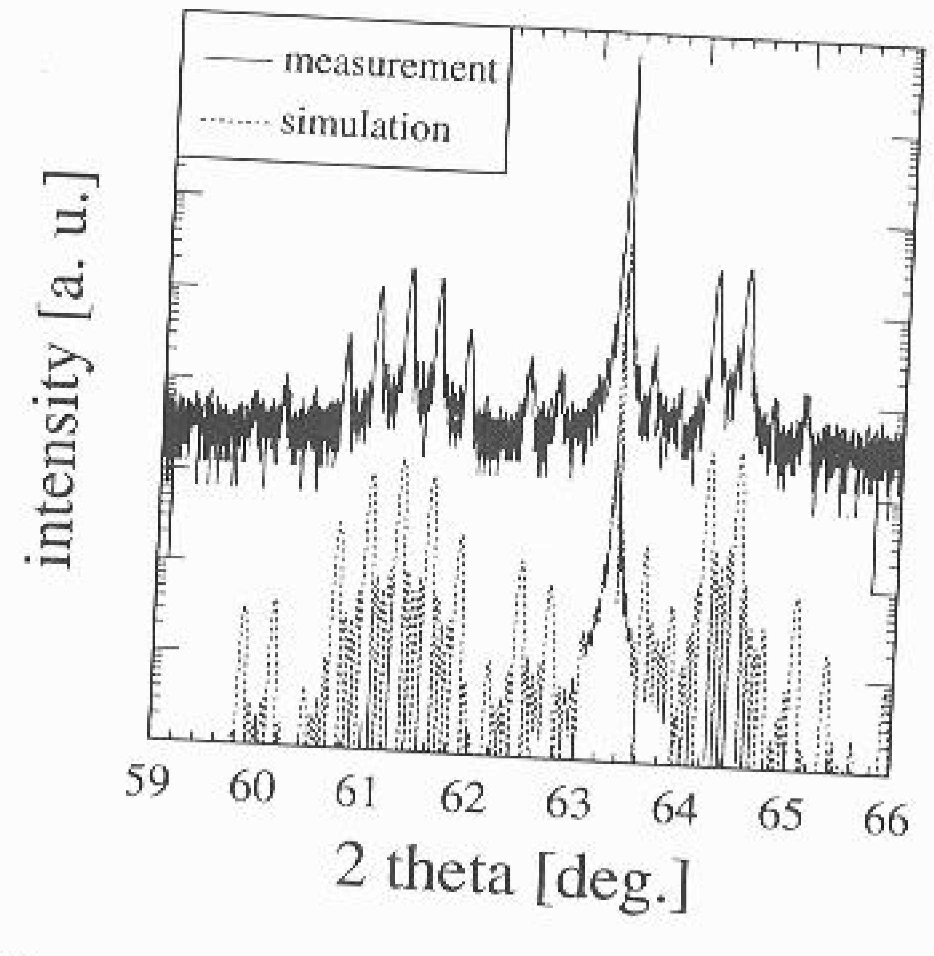

Figure 2: X-ray diffraction spectra (400) of a strain-symmetrized MQW structure (5 periods) with 1 µm $In_{0.52}Al_{0.48}As$ buffer layer on InP substrate (barrier: 23.8 nm $In_{0.53}Al_{0.47}As$, QW: 12.0 nm $In_{0.749}Ga_{0.251}As$; solid: measurement, dotted: dynamical scattering theory).

E on (100) oriented InP:Fe substrates
re of 530 °C and a V/III ratio (beam
f the ternary layers were obtained by

sequence of the investigated HEMT
ck $In_{0.52}Al_{0.48}As$ layers and two
ratures of the Ga effusion cell was
r from the value necessary for lattice
QW. The In flux was kept constant,
s our MBE machine is equipped with
ere able to grow the layer sequence
QW interfaces, having different Al

QWs and the barriers are given in
yer was 1.5×10^{19} cm^{-3} for sample
all others. The measured transport
ction in the cap layers: Samples
ss, whereas the other samples have
ped InGaAs). The doping in the cap

made by Hall measurements at 300,
nts at 4.2 K to separate the 2DEG
ers. The thicknesses of the surface

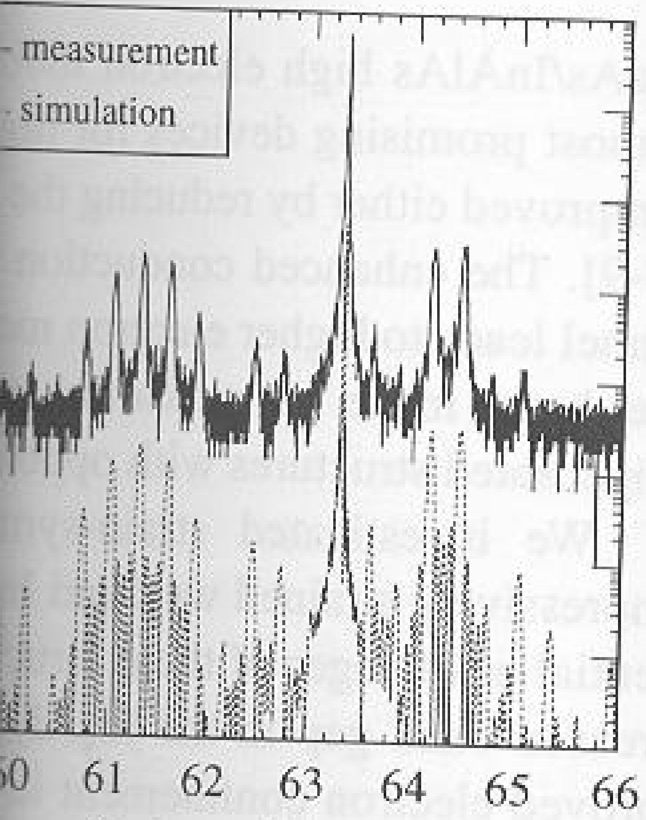

-ray diffraction spectra (400) of a
trized MQW structure (5 periods) with
$_{0.48}As$ buffer layer on InP substrate
8 nm $In_{0.53}Al_{0.47}As$, QW: 12.0 nm
As; solid: measurement, dotted:
ttering theory).

near layers were controlled by X-ray reflectivity measurements (XRR). Compositions of the strained layers were monitored by X-ray diffraction (XRD) on strain-symmetrized MQW structures, always grown in direct sequence with the HEMT structures.

3. Structural and transport properties

Figure 2 shows the XRD spectra of a strain-symmetrized $In_{0.74}Ga_{0.26}As/In_{0.415}Al_{0.585}As$ MQW structure. The nominal layer sequence is a 1 μm thick lattice matched $In_{0.52}Al_{0.48}As$ buffer layer, followed by 5 QWs, having 24 nm thick $In_{0.415}Al_{0.585}As$ barriers and 12 nm wide $In_{0.74}Ga_{0.26}As$ wells. The simulated spectrum using dynamical scattering theory fits the measured curve excellently, with only small deviations from the nominal values. The compositions and thicknesses from the simulation are: 23.8 nm $In_{0.419}Al_{0.581}As$, 12.0 nm $In_{0.749}Ga_{0.251}As$, 1 μm $In_{0.522}Al_{0.478}As$ buffer. Although we used high growth temperatures of 530 °C and a wide range of In contents from 0.415 to 0.74 in the QW and the barriers, the simulation indicates that there is no noticable In segregation at the interfaces, in contrast to observed segregation lengths of 3.5 nm at the interfaces of pseudomorphic $In_{0.74}Ga_{0.26}As/In_{0.52}Al_{0.48}As$ MQWs with lattice matched barriers, which were grown under identical growth conditions [13]. In segregation has also been reported for the growth of strained InGaAs layers on GaAs [10-12].

Table I: Structural parameters, mobilities and 2-DEG densities of strain-symmetrized $In_xGa_{1-x}As/In_yAl_{1-y}As$ HEMT structures with different In-content in the channel and the barriers (QW thickness: 12 nm)

Sample	LM ssd M5406	PM ssd M5407	PM ssd M5408	SS ssd M5420	SS ssd M5421	PM ssd M5409	SS ssd M5424	PM dsd M5410	SS dsd M5425
x ($In_xGa_{1-x}As$) QW	0.53	0.67	0.74	0.67	0.74	0.74	0.74	0.74	0.74
y ($In_yAl_{1-y}As$) Barrier	0.52	0.52	0.52	0.45	0.415	0.52	0.415	0.52	0.415
doping N_D [10^{19} cm^{-3}]	1.0	1.0	1.0	1.0	1.0	1.5	1.5	1.0	1.5
μ_{Hall}(300K) [cm^2/Vs]	9420	11390	12220	11040	12150	11090	11150	7450	7640
n_{Hall}(300K) [$10^{12}cm^{-2}$]	3.16	3.36	3.49	3.72	3.82	4.22	4.56	6.58	7.67
μ_{Hall}(77K) [cm^2/Vs]	30960	43000	50220	43150	50070	40700	46860	14160	16280
n_{Hall}(77K) [$10^{12}cm^{-2}$]	3.03	3.21	3.35	3.53	3.67	4.05	4.25	6.55	7.31
μ_{Hall}(4.2K) [cm^2/Vs]	33540	54940	62930	46820	-	54970	51080	16230	15060
n_{Hall}(4.2K) [$10^{12}cm^{-2}$]	2.79	2.97	3.18	3.79	-	3.64	4.30	6.07	6.92
$n_{1,SdH}$(4.2K) [$10^{12}cm^{-2}$]	2.55	2.68	2.74	2.81	-	3.05	3.12	3.84	4.15
$n_{2,SdH}$(4.2K) [$10^{12}cm^{-2}$]	0.26	0.38	0.45	0.46	-	. 0.61	0.69	2.20	2.55

LM=lattice matched QW and barriers; PM=pseudomorphic QW; SS=strain-symmetrized structure
ssd=single-sided doping in top barrier; dsd= double-sided doping in both barriers

The transport properties of all the HEMT structures investigated in the course of this work are given in Table I. Sample M5406 is a lattice matched reference sample with the QW width of 12 nm used in all our HEMT structures. The mobilities of this reference structure were measured to 9400 cm^2/Vs and 33500 cm^2/Vs at 300 and 4.2 K, respectively. These mobilities are clearly lower than those obtained on lattice matched structures with 32 nm wide QWs (10000 cm^2/Vs and 42000 cm^2/Vs) due to increased interface roughness scattering by the bottom barrier.

Using compressive strain only in the QWs, i.e with lattice matched barriers, increases the mobilities with rising In content from 11400 cm^2/Vs and 55000 cm^2/Vs for $x = 0.67$ (sample M5407) to 12200 cm^2/Vs and 63000 cm^2/Vs for $x = 0.74$ (sample M5408). Simultaneously there is an increase in the 4.2 K 2DEG densities from 2.81×10^{12} cm^{-2} to 3.06×10^{12} cm^{-2} and 3.19×10^{12} cm^{-2} (samples M5406, M5407 and M5408). SdH measurements clearly show two occupied subbands with densities n_1 and n_2. The intersubband separation in sample M5406 was found to be 108 meV by the peak separation in photoluminescence, agreeing well with the observed values of n_1 and n_2 using the calculated density of states.

On increasing the doping level to 1.5×10^{19} cm^{-3} in the supply layer, the total 2DEG density reaches 3.66×10^{12} cm^{-2}, while still maintaining a 4.2 K mobility of 55000 cm^2/Vs (sample M5409, lattice matched barriers, single-sided doping). Using $In_yAl_{1-y}As$ barriers under tensile strain increases the carrier density even further. Sample M5424 is strain-symmetrized with $x = 0.74$ in the QW and $y = 0.415$ in the barriers, showing a total 2DEG density of 3.81×10^{12} cm^{-2} at 4.2 K. The mobilities are practically unchanged (see Table I).

A further increase of the In content in the QW to $x = 0.78$ with a corresponding decrease in the barrier to $x = 0.34$, however, resulted in a drastic decrease in mobility due to

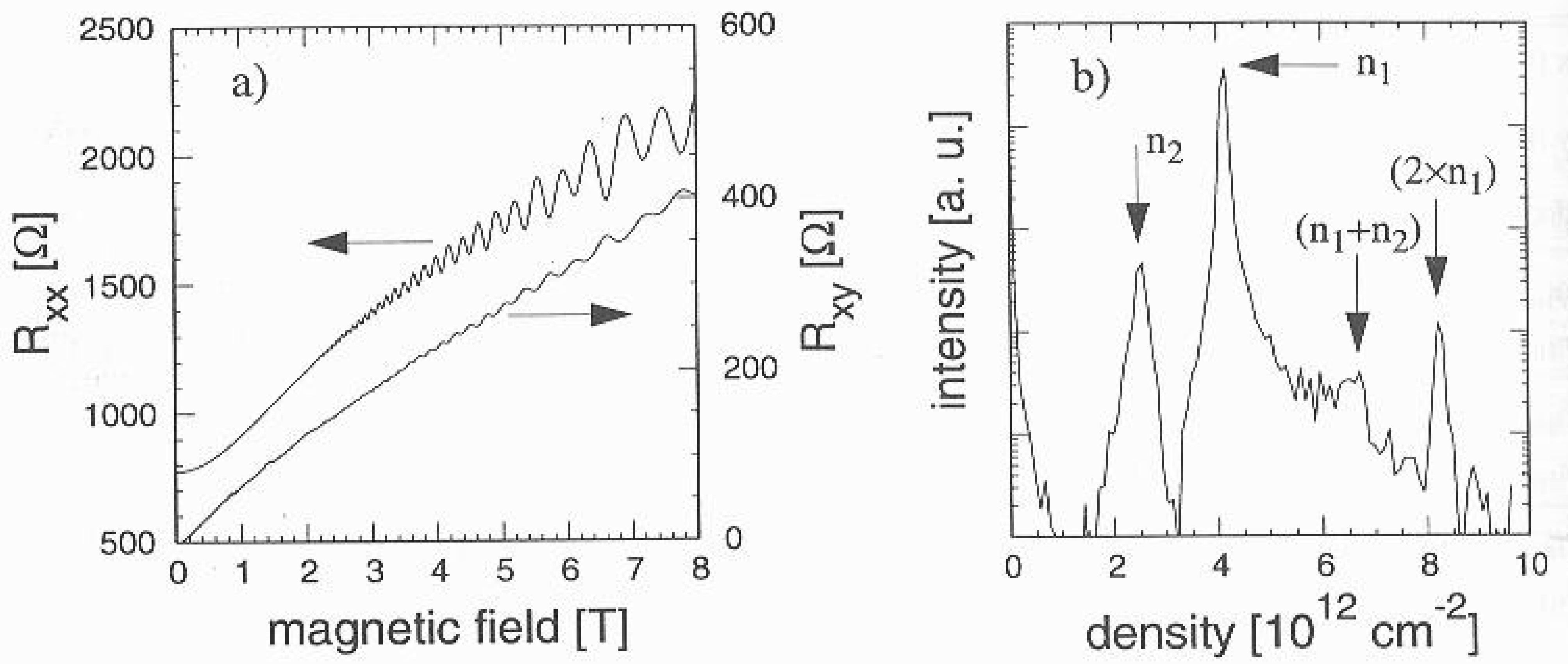

Figure 3: a) Shubnikov-de Haas measurement on a strain-symmetrized HEMT structure with double-sided doping (sample M5425); b) Fourier transformation of R_{xx}.

relaxation and the formation of misfit dislocations. Whereas it has been reported [8] that the critical In content of strained InGaAs QWs could be increased by the insertion of stress compensating layers, our results show that, under our growth conditions, the maximum In content is the same in pseudomorphic and strain-symmetrized structures.

Extremely high 2DEG densities were, however, obtained using double-sided doping from both - top and bottom - barriers. Total 2DEG densities as high as 6.04×10^{12} cm^{-2} and 6.70×10^{12} cm^{-2} were found by SdH measurements at 4.2 K in samples M5410 and M5425, respectively. The first sample is doped to 1.0×10^{19} cm^{-3} in the supply layer with a bottom spacer of 4 nm, the corresponding values for the latter are 1.5×10^{19} cm^{-3} and 6 nm. These 2DEG densities are, to our knowledge, the highest ever reported for InGaAs/InAlAs HEMTs. The marked reduction in mobility of double-sided doped structures in comparison to single-sided doping is due to Si segregation towards the channel [14]. So, for example in structure M5425 we found mobilities of 7600 cm^2/Vs and 15100 cm^2/Vs at 300 and 4.2 K, respectively. In spite of the low mobility and considerable parallel conduction in the cap layer we were able to determine clearly the separate densities of the two occupied subbands by SdH measurements and Fourier transformation, as shown in Fig. 3. This analysis yields densities of 4.15 and 2.55×10^{12} cm^{-2} for the first and the second subband in the QW.

4. High electron mobility transistors

HEMT devices with a gate length of 0.13 μm were fabricated from sample M5406 - M5408, using e-beam lithography and wet chemical selective gate recess with succinic acid. The increasing In content from x = 0.53 to 0.74 in the active QW (the barriers of these samples were lattice matched to the InP substrate) resulted in an increase in the extrinsic transconductance from 670 mS/mm to 1150 mS/mm, with a concurrent increase in the intrinsic values from 1000 mS/mm to 1600 mS/mm. The cut-off frequencies for the current gain were measured to 200 - 220 GHz for all devices.

5. Summary

Single-sided doped strain-symmetrized $In_{0.74}Ga_{0.26}As/In_{0.415}Al_{0.585}As$ HEMT structures showed 2DEG densities as high as 3.81×10^{12} cm^{-2} and mobilities of 51100 cm^2/Vs at 4.2 K. Extremely high 2DEG densities of 6.70×10^{12} cm^{-2} were obtained using double-sided doping from both barriers. XRD of strain-symmetrized MQW structures showed that the segregation of In at the interfaces was significantly suppressed by strain-symmetrization.

6. Acknowledgement

We thank the German Federal Ministry of Research and Technology (BMFT) and Siemens AG for financial support under contract 01 BM 118/6.

References:

[1] Enoki T, Tomizawa M, Umeda Y and Ishii Y 1994 Jpn. J. Appl. Phys. 33 798-803

[2] Chough K B, Chang T Y, Feuer M D, Sauer N J and Lalevic B 1992 IEEE Electron Device Lett. 13 451-453

[3] Nguyen L D, Brown A S, Thompson M A and Jelloian L M 1992 IEEE Trans. Electron Devices 39 2007-2013

[4] Gueissaz F, Enoki T and Ishii Y 1993 Electron Lett. 29, 2222-2223

[5] Hwang K C, Ho P, Kao M Y, Fu S T, Liu J, Chao P C, Smith P M and Swanson A W 1994 Proc. of the 6th Intern. Conf. on Indium Phosphide and Rel. Mat. (Santa Barbara, California, USA, March 27-31, 1994) 18-20

[6] Tacano M, Sugiyama Y and Takeuchi Y 1991 Appl. Phys. Lett. 58 2420-2422

[7] Brown A S, Schmitz A E, Nguyen L D, Henige J A and Larson L E 1994 Proc. of the 6th Intern. Conf. on Indium Phosphide and Rel. Mat. (Santa Barbara, California, USA, March 27-31, 1994) 263-266

[8] Chin A, and Chang T Y 1990 J. Vac. Sci. Technol. B8 364-366

[9] Hong W-P, Ng G I, Bhattacharya P K, Pavlidis D and Willing S 1988 J. Appl. Phys. 64 1945-1949

[10] Toyoshima H, Niwa T, Yamazaki J and Okamoto A 1993 Appl. Phys. Lett. 63 821-823

[11] Kao Y C, Celii F G and Liu H Y 1993 J. Vac. Sci. Technol. B11 1023-1026

[12] Muraki K, Fukatsu S and Shiraki Y 1992 Appl. Phys. Lett. 61 557-559

[13] Klein W, Böhm G, Heiß H, Kraus S, Xu D, Semerad R, Tränkle G and Weimann G 1994 Proc. of the 8th Intern. Conf. on Molecular Beam Epitaxy (Osaka, Japan, Aug. 29 - Sep. 2, 1994), to be published in J. Crystal Growth

[14] Brown A S, Metzger R A, Henige J A, Nguyen L, Liu M and Wilson R G 1991 Appl. Phys. Lett. 59 3610-3612